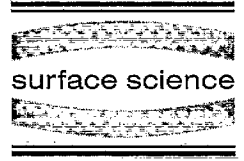




ELSEVIER

Surface Science 369 (1996) 360–366



# Simulated growth of layers on a substrate with mismatch: structural studies

S. Tan <sup>a</sup>, A. Ghazali <sup>b,\*</sup>, J.C.S. Lévy <sup>a</sup>

<sup>a</sup> *Laboratoire de Magnétisme des Surfaces, Université Paris 7 – Denis Diderot, 75251 Paris 5, France*

<sup>b</sup> *Groupe de Physique des Solides, C.N.R.S., URA 17, Université Paris 7 – Denis Diderot and Université Paris 6 – P. et M. Curie, 75251 Paris 5, France*

Received 14 April 1996; accepted for publication 11 July 1996

## Abstract

High temperature deposition of metallic materials on a (111) face of a fcc substrate, followed by a slow cooling down to a given temperature, is simulated by means of a Monte-Carlo algorithm with Lennard-Jones interatomic pair potentials. Adsorption and growth modes on the surface are studied in order to determine whether the growth is three- or two-dimensional, according to relevant parameters such as lattice mismatch and relative atomic binding energy. For a  $\pm 10\%$  mismatch it is found that the Stranski–Krastranov process starts early and is later healed by the appearance of bridges between islands, after a deposition of about ten monolayers. The interlayer distance undergoes oscillations as a function of the layer number. This is observed for a  $\pm 10\%$  mismatch as well as for a 5% mismatch.

*Keywords:* Computer simulations; Growth; Single crystal epitaxy; Surface structure

## 1. Introduction

The recent progress in surface sciences [1] and in ultra high vacuum technology along with the development of numerous high resolution surface microscopy techniques enable physicists to design new materials such as metallic multilayers with rich potential applications, such as, for example, magnetic devices with giant magnetoresistance [2]. The details of the crystallographic structure of magnetic–non-magnetic multilayers is quite important for such experiments [2,3] because magnetic pinholes and bridges can shortcut the indirect Ruderman–Kittel–Kasuya–Yosida (RKKY) mag-

netic coupling through non-magnetic layers [4]. More generally, the details of the structure at the interface are very important for nanostructures such as quantum wells, quantum wires and quantum dots. Recent observations of multilayer structures by means of synchrotron X-radiation has provided evidence that interface roughness depends on thermal annealing [5]. Thus simulation of layer growth is useful in order to shed light on the physical conditions of roughness and of the formation of atomic bridges through different layers. In the case of magnetic–non-magnetic–magnetic multilayer structures this means a shortcut of the expected RKKY coupling through the non-magnetic layer. The goal of the present paper is to simulate the deposition and growth of atomic layers with and without lattice mismatch on a

\* Corresponding author. Fax: +33 01 435 428 78;  
e-mail: ghazali@gps.jussieu.fr

substrate, in order to study the structure of the adsorbate according to the lattice mismatch. Here we take as a substrate a fixed triangular lattice simulating, for instance the (111) face of a fcc lattice.

Two different sizes of the fixed substrate are considered in order to account for size effects: samples of sizes  $30 \times 30$  and  $50 \times 50$ , both with free boundaries. Periodic boundary conditions are not used here since they may induce spurious superstructure orderings of periods commensurate with the considered size. The free boundaries induce defects and local rearrangements in the vicinity of the boundary. These particular structures are easily recognized and will not be considered in the present analysis.

This paper focuses on the simulation of the deposition of stable structures by means of a Monte-Carlo technique. First a random configuration of adatoms of about one monolayer coverage is computed, with adatoms randomly cast in a box of one interatomic distance thick, above the substrate. Then this high temperature liquid-like deposit is relaxed by means of a Monte-Carlo simulation. Lennard-Jones (LJ) potentials are used both for adatom–adatom (aa) pairs and for adatom–substrate atom (as) pairs to derive the relaxation process at the surface, while the interaction between fixed substrate atoms (ss) does not take part in this process. Even if the standard (6,12) LJ potentials can be improved in several ways to describe a more realistic metallic binding with fitted binding energy, lattice parameter and elastic moduli [6], the present calculation already gives the principle of a general approach. More specific studies including generalized ( $n,m$ ) LJ potentials [7], use two effective exponents,  $nm$  and  $m$ :

$$V_{n,m}(q) = \epsilon \frac{q^n - nq}{n-1} \text{ with } q = (\sigma/r)^m. \quad (1)$$

In the present approach, very simple basic cases are studied. First, the binding energy between an adatom and a substrate atom is assumed to be equal to the binding energy between adatoms in a pair:  $E_{aa} = E_{as}$ . Three adatom sizes are considered: (i) without mismatch ( $\sigma_{aa} = \sigma_{ss}$ ), (ii) with a  $\pm 10\%$  mismatch and adatoms smaller or larger than the

substrate atoms ( $\sigma_{aa} = 0.9\sigma_{ss}$ ,  $\sigma_{aa} = 1.1\sigma_{ss}$ ), and (iii) with a 5% mismatch and adatoms smaller than the substrate atoms ( $\sigma_{aa} = 0.95\sigma_{ss}$ ).

An initial random configuration of adatoms is chosen before applying a Metropolis algorithm. At a given temperature,  $T$ , each atom is visited and allowed to move randomly with a uniform probability within a small cube of side of  $b$  around the initial position. The size  $b$  is chosen to be small in front of the interatomic distance and is taken as being proportional to the square root of the temperature in order to optimize the computation as a function of thermal fluctuations. The cubic shape with standard axes is only used for the convenience of a random sampling. The atomic interaction energies before and after moving are compared. The final position is accepted or rejected according to the Boltzmann probability:  $p = \exp(-\Delta E_i/kT)$  where  $\Delta E_i$  is the energy difference for atom  $i$  in two successive configurations. The total energy  $E_T$  is computed after a real or virtual motion of every adatom. After several thousand such steps,  $E_T$  is observed to fluctuate around a steady value [8] when thermal equilibrium is reached.

Adatoms are deposited at the temperature  $T$  when  $k_B T/E_{aa} = 0.3$ , which is close to but lower than the melting temperature. About one hundred thousand Monte-Carlo steps are performed in order to obtain the equilibrium at the initial temperature. Then the system is cooled down to  $2T/3$ , and later to  $T/3$ . After reaching the equilibrium at a given temperature, further depositions are made with the same amount of new adatoms and the same process is continued until 16 monolayers are deposited.

## 2. The first adlayers

In the case of no mismatch, as seen in Fig. 1, the first top layer is divided into two symmetric domains, separated by a domain boundary, i.e. a line. In the left hand side domain, the adatoms lie on triangles pointing upwards. In the right hand side domain, the reverse is the case. The growth mode is two-dimensional for the first and second adlayers. In the second adlayer, domains with a fcc structure – ABC stacking – and domains with

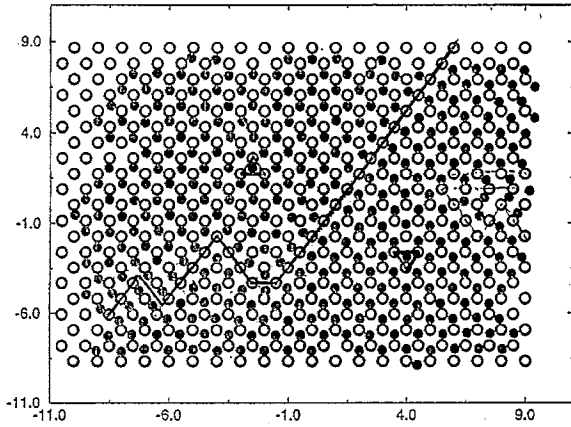


Fig. 1. Monolayer of adatoms (black circles) without mismatch on a  $20 \times 20$  triangular lattice as a substrate (open circles). A wall, shown by the solid line, divides the monolayer into two symmetric parts, left and right; adatoms lie on triangles pointing upwards and downwards, respectively.

an hexagonal structure – ABA stacking – coexist. Such an unlifted degeneracy occurs because the fixed substrate is a single monolayer which does not induce any preferential stacking and because of the well known fcc–hcp quasi-degeneracy for Lennard-Jones interactions [9]. The boundary between the two domains of the first layer also appears in the second layer, and also separates hcp and fcc domains.

In the case of a 10% mismatch with smaller adatoms, as seen in Fig. 2, the first adlayer forms

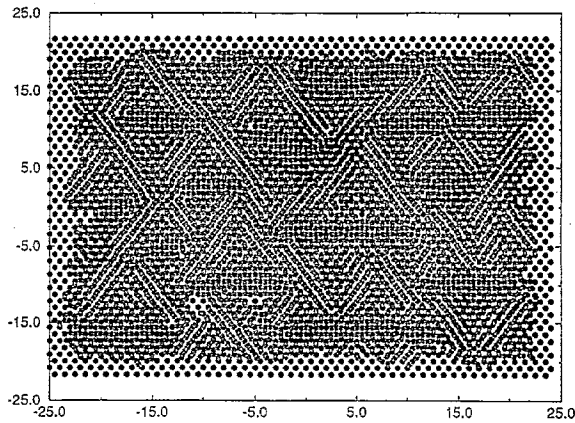


Fig. 2. Commensurate superstructure formed by a monolayer of small adatoms (grey circles) with a  $-10\%$  mismatch on a  $50 \times 50$  rigid triangular lattice as substrate (black circles).

a structure which is commensurate with the substrate, with a superperiod of about ten substrate–substrate atomic distances. Generally, in the case of a mismatch of  $\pm 1/n$ , i.e. when the bulk lattice parameters  $a$  and  $a'$  fulfill the condition  $a' = (1 \pm 1/n)a = ((n \pm 1)/n)a$ , the commensurate period is  $na' = (n \pm 1)a$ . For instance in the case of a  $5\%$  mismatch  $n=20$ , and an approximate commensurate structure with a superperiod of about twenty substrate–substrate distances is observed in the deduced structure shown in Fig. 3. Thus the larger the mismatch, the smaller the superperiod. It should be emphasized that such a commensurate structure also modulates point defects such as vacancies and clusters of vacancies which are located at places where nearest adatoms would bear only a weak tension. This usual rule holds for one-dimensional commensurate structures [10]. A careful analysis of this superstructure also shows larger-scale defects in the arrangement of upwards and downwards domains. Here such defects originate from the free boundary conditions.

### 3. Subsequent adlayers and the Schwoebel barrier

With a  $\pm 10\%$  mismatch, growth is two-dimensional in the first two layers. However, for subsequent layers, in the case of small adatoms, i.e. a  $-10\%$  mismatch, further growth is three-dimensional [1,11]. In the case of a positive mismatch

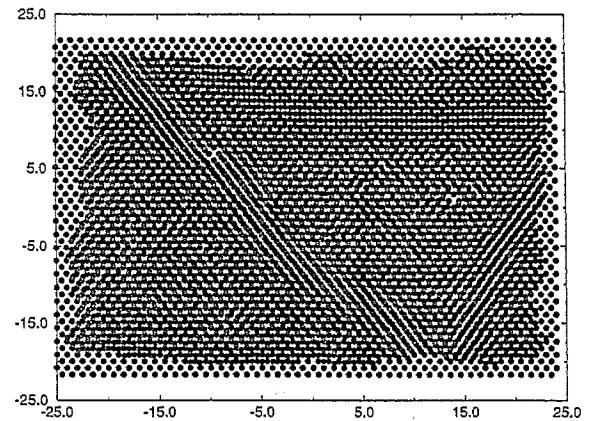


Fig. 3. Same as Fig. 2 but with  $-5\%$  mismatch.

the growth is two-dimensional for the first five layers. Fig. 4 shows islands grown on a  $30 \times 30$  lattice, with a  $-10\%$  mismatch. On a  $50 \times 50$  substrate lattice, quite similar patterns occur during simulated growth. The growing layers retain a memory of the structure beneath, and point defects such as vacancies in the first adatom layer initiate island boundaries in subsequent layers. The lateral size of the islands increases as the inverse of the mismatch [1]. This is a consequence of the period of the surstructure which is approximately equal to the lateral size of the islands. The top layer displayed in Fig. 4 shows triangular shaped islands, in accord with other observations [11,12]. This layer also shows the occurrence of numerous local rotations from the substrate orientation. Such local rotations are also observed experimentally in some cases [13], such as the moiré patterns observed by scanning tunnelling microscopy (STM).

The island formation is linked with the existence of vacancies. At a given stage of growth, vacancies are formed in the last deposited layer, the third one in the case of a  $-10\%$  mismatch. Then the potential energy of a fictitious test atom moving over a terrace, in the vicinity of a vacancy, gives a measure of the effective Schwoebel barrier [14] to diffusion when the fictitious atom trajectory crosses the vacancy. Such a calculation is reported in

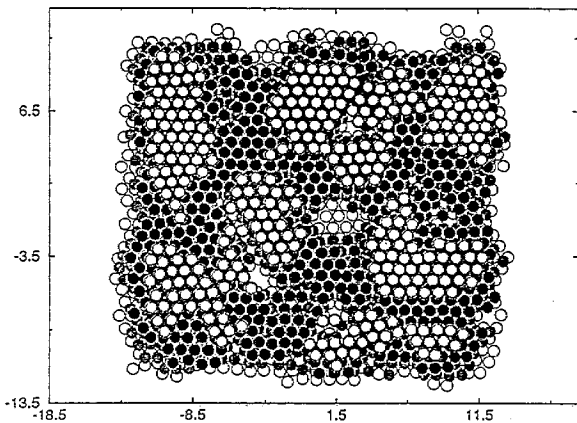


Fig. 4. Second (open circles), third (grey circles), fourth (black circles) and fifth (white opaque circles) adlayers. Mismatch =  $-10\%$ . The substrate is  $30 \times 30$ . The substrate and first layer are not shown.

Fig. 5b for the case where the atom trajectory first crosses a hcp terrace and then a small valley before crossing a fcc terrace, as shown by the line C in Fig. 5a. The fictitious atom is maintained at one interplane distance above successive terraces during the whole trajectory. Fig. 5 shows very high Schwoebel barriers on both sides of the vacancy which points out that growth starts to be three-dimensional.

During growth, new adatoms diffuse towards "perfect crystal" areas of the top layer and join these areas rather than filling holes in the lowest adatom layers. At a given stage and temperature of deposition, no island reorganization occurs in the gaps between islands. The size of one particular island depends on the degree of perfection of the layer just beneath and is slightly smaller than the size of the previous one. Except for a few isolated adatoms, the structure of the top layer is quite smooth, as shown in Fig. 4.

In Fig. 6 the adatom distribution is plotted as a function of the distance from the adatom to the substrate in the case of a  $-10\%$  mismatch, providing evidence for well defined layers. Starting from the substrate, the number of adatoms in each layer regularly decreases by about  $5\%$  per layer, as shown in the insert of Fig. 6. This means that islands have quite a steep slope and an extrapolated maximum height of about twenty layers. The last five or six layers show a more irregular shape; they define the observed uppermost roughness. Such a process ends when a further deposit starts to increase the amount of adatoms in the top layer of present islands. The latter process seems to start after the twelfth layer deposit as can be seen in Fig. 6. Then, bridges of adatoms start to connect previously isolated islands as soon as more adatoms are deposited. The connected pattern grows within the uppermost layer and, after invading the whole sample, a new bidimensional growth mode is expected.

During growth, numerous strains and twists appear within the islands. As a result, the interlayer distance shows an oscillating behaviour as a function of the layer number for a  $\pm 10\%$  mismatch. The relative fluctuation amplitude is as large as  $2\%$ . Similar oscillating behaviour has also been observed with a  $5\%$  mismatch with a smaller

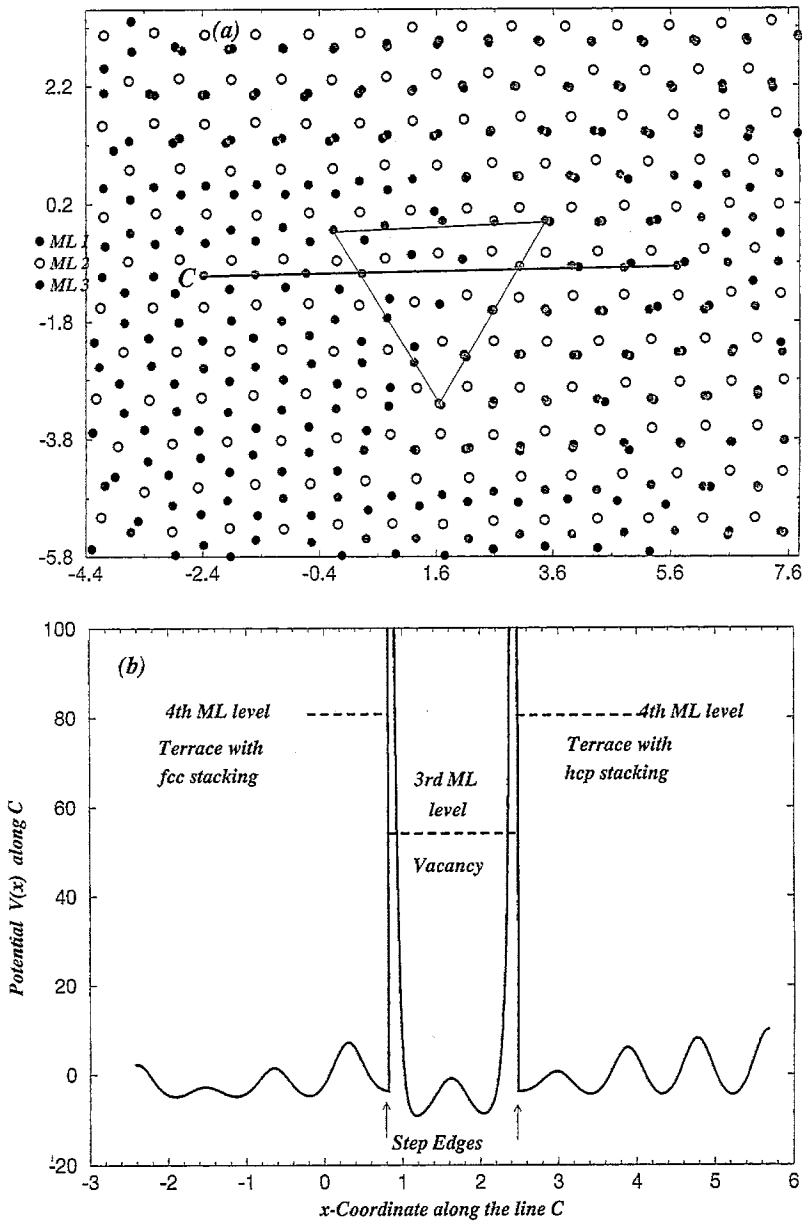


Fig. 5. (a) Portion of the sample of Fig. 4 with a  $-10\%$  mismatch, showing a vacancy in the third adlayer. (b) Potential energy as a function of the position of a fictitious atom moving along a path projected on the line C. Very high Schwoebel barriers appear on both sides of the vacancy.

amplitude (1%). When considering only adatoms within a narrow column with a few atoms in each layer, the average interlayer distance within these sampled columns also shows an oscillating behaviour as a function of the layer number. This is

displayed in Fig. 7 for  $-5\%$  and  $-10\%$  mismatches. We would point out that this generic feature of interlayer distance oscillations does not occur in the case of a one dimensional model which can be easily solved numerically with various boundary

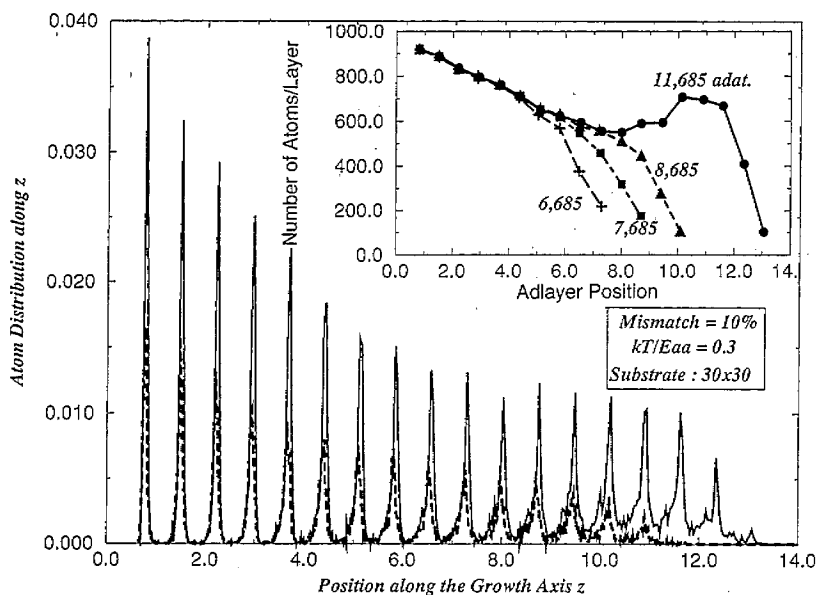


Fig. 6. Adatom distribution as a function of the distance from the substrate after deposition of 11,685 adatoms (solid line) and 9,681 adatoms (dashed line). The distribution scales are different for clarity. Insert: Number of adatoms per monolayer after successive deposits; the corresponding total numbers of deposited adatoms are indicated. The lines are a guide to the eye. The substrate:  $30 \times 30$ , mismatch =  $-10\%$  and  $T = 0.3E_{aa}/k_B$ .

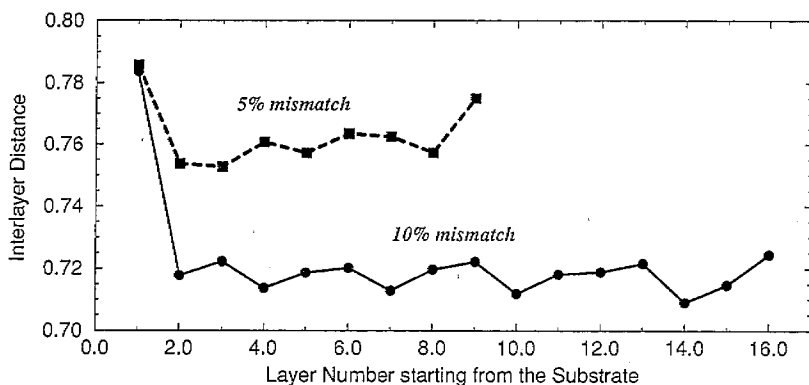


Fig. 7. The  $(n-1, n)$  interlayer distance as a function of the layer number  $n$  for a  $-5\%$  and  $-10\%$  mismatch. Distances are given in substrate interatomic spacing units. The lines are only drawn to guide the eye and emphasize the oscillations.

conditions. The probable reason for such oscillations lies in the interplay between numerous local tridimensional rotations of groups of atoms within the Stranski–Krastanov islands. It is by means of such rotations that the layer configuration is relaxed. The experimental observations of moiré patterns [13] corroborate this explanation.

The difference between samples obtained after

cooling down to the temperature  $k_B T = 0.1E_{aa}$ , and samples annealed at higher temperature,  $k_B T = 0.3E_{aa}$ , is not significant on the above mentioned statistical basis. However, at low temperatures the islands tend to separate, and the bridges between neighbouring islands to break, while their shape seems to be more geometrical with sharp edges.

When a harder Lennard-Jones potential, i.e. with a repulsive exponent larger than twelve is used, crystallites are formed from the first layer onwards, already with a 5% mismatch. This leads to an imperfectly covered substrate. Conversely, with a five per cent mismatch, when the adatom–adatom interaction dominates the adatom–substrate atom interaction ( $E_{aa} = 1.5E_{as}$ ) the growth mode up to four layers always seems to be two-dimensional, i.e. this condition achieves a strong wetting situation.

#### 4. Conclusion

The 2D–3D (Stranski–Krastanov) growth mode seems to be a general rule in the Lennard-Jones model of growth on (111) metal surfaces with a large enough lattice mismatch. Thus the possibility of magnetic bridges through non-magnetic layers seems to be greatest when the number of non-magnetic layers is less than twenty, i.e. before the definite healing of the partition into islands. The island shape certainly depends on the early history of the adsorption process. Our present model simulates an initial liquid-like deposit which crystallizes during the adsorption process. Of course the use of smaller amounts of deposit would enable us to simulate vapour deposition, and more realistic potentials should give more accurate results. However, we believe that the present model already points out some of the main features of layer growth on a substrate with a lattice mismatch, e.g. the local crystalline quality of the deposit, the occurrence of Stranski–Krastanov islands and non-negligible fluctuations in the interadlayer distance.

#### Acknowledgements

Part of this work was done within the framework of contract CHRX-CT93-0320 of the European Economic Community and reported at the 2nd International Symposium on Metallic Multilayers held in Cambridge, UK, 11–14 September 1995. A grant from the Comité Français de Physique is warmly acknowledged.

#### References

- [1] A. Zangwill, *Physics at Surfaces* (Cambridge University Press, Cambridge, 1988); M.C. Desjonquères and D. Spanjaard, *Concepts in Surface Physics* (Springer, Berlin, 1993).
- [2] P.M. Levy, *Solid State Phys.* 47 (1994) 367.
- [3] M.N. Baibich, J.M. Broto, A. Fert, F. Nguyen Van Dau, F. Petroff, P. Etienne, G. Creuzet, A. Friedrich and J. Chazelas, *Phys. Rev. Lett.* 61 (1988) 2472.
- [4] D. Mercier, J.C.S. Lévy, J.S.S. Whiting, M. Watson and A. Chambers, *Phys. Rev. B* 43 (1991) 3311; D. Mercier and J.C.S. Lévy, *J. Magn. Magn. Mater.* 139 (1995) 240; 145 (1995) 133.
- [5] H. Laidler, B.J. Hickey, T.P.A. Hase, B.K. Tanner and R. Schad, *J. Magn. Magn. Mater.* (1996), to be published.
- [6] A.P. Sutton and J. Chen, *Philos. Mag. Lett.* 61 (1990) 139; M.H. Grabow and G.H. Gilmer, *Surf. Sci.* 194 (1988) 333; T.J. Raeker and A.E. De Pristo, *Surf. Sci.* 248 (1991) 134.
- [7] S. Tan, A. Ghazali and J.C.S. Lévy, in preparation.
- [8] A. Ghazali and J.C.S. Lévy, in: *Aperiodic 94*, Eds. G. Chapuis and W. Paciorek (World Scientific, Singapore, 1995) p. 164.
- [9] T. Kihara and S. Koba, *J. Phys. Soc. Jpn.* 7 (1952) 348.
- [10] F.C. Frank and J.H. Van der Merwe, *Proc. R. Soc. A* 198 (1949) 205; 200 (1949) 125; S. Aubry, *J. Phys. (Paris)* 44 (1983) 147.
- [11] For a review, see: J.A. Venables, G.D.T. Spiller and M. Hanbucker, *Rep. Prog. Phys.* 47 (1984) 399.
- [12] S. Liu, Z. Zhang, G. Comsa and H. Metiu, *Phys. Rev. Lett.* 71 (1993) 2967.
- [13] T. Wiederholt, H. Brune, J. Wintterlin, R.J. Behm and G. Ertl, *Surf. Sci.* 324 (1995) 91.
- [14] R.L. Schwoebel, *J. Appl. Phys.* 40 (1969) 614.